Electronic Supplementary Information

Controlling the magnetic properties of dysprosium metallofullerene within metal-organic framework

Yongjian Li,[a,b] Taishan Wang,*[a] Haibing Meng,[a,b] Chong Zhao,[a] Mingzhe Nie,[a,b] Li Jiang,[a] Chunru Wang*[a]

[a.] Beijing National Laboratory for Molecular Sciences, Key Laboratory of Molecular Nanostructure and Nanotechnology, Institute of Chemistry, Chinese Academy of*Science, Zhongguancun North First Street 2,100190 Beijing, China*

E-mail: wangtais@iccas.ac.cn; crwang@iccas.ac.cn

[b.] University of Chinese Academy of Sciences, Beijing 100049, China

Table of contents

1. Synthesis and Characterization Methods

1-1. Synthesis of $DySc_2N@C_{80}$

$DySc_2N@C_{80}$ was synthesized by arc-discharging method. Briefly, the mixture of graphite powder, Sc/Ni alloy and $Dy(NO_3)_3 \cdot 5H_2O$ powder with a mass ratio of 1:3:6 was packed into core-frilled graphite rods. Subsequently the rods were burnt in a Krätschmer–Huffman generator under an atmosphere of 6 Torr N_2 and 194 Torr He. The as-prepared soot was Soxlet-extracted with toluene for 12 h. $DySc_2N@C_{80}$ was isolated and purified by multi-step high performance liquid chromatography (HPLC).

1-2. Synthesis of C_4H_9N-$DySc_2N@C_{80}$

$DySc_2N@C_{80}$ in toluene solution was heated with N-ethylglycine and paraformaldehyde at 120 °C for 50 min to give corresponding fulleropyrrolidine with yield of nearly 70%. Pure C_4H_9N-$DySc_2N@C_{80}$ was isolated by HPLC.

1-3. Synthesis of MOF-177

MOF-177 was prepared by the solvothermal method as previously reported.[1] Briefly, 60 mg of $Zn(NO_3)_2 \cdot 6H_2O$ and 40 mg of H_3BTB were dissolved in 10 ml of DEF, then the solution was sealed in a reaction vessel and heated at a rate of 2 °C/min to 85 °C and held for 48 h, and cooled at a rate of 2 °C/min to the room temperature. The as-synthesized crystals were rinsed three times with toluene.

1-4. Preparation of $DySc_2N@C_{80}$@MOF-177 and C_4H_9N-$DySc_2N@C_{80}$@MOF-177

About 10 mg of MOF-177 crystals were immersed in a solution 0.1 mg, 0.3 mg and 0.5 mg of $DySc_2N@C_{80}$ in toluene for 7 days respectively until the color of the crystals changed to orange. The crystals with different contents of $DySc_2N@C_{80}$ were washed with toluene (5 × 10 ml) and dried under N_2 flow. C_4H_9N-$DySc_2N@C_{80}$@MOF-177 with different contents of C_4H_9N-$DySc_2N@C_{80}$ was prepared according to the same processes.

1-5. Characterizations methods of materials and magnetism

TEM images and element mapping analysis were characterized by a JEOL 1011 instrument. PXRD was performed on the Thermo Scientific ESCALab 250Xi using 200 W monochromated Al Kα radiation. The content of $DySc_2N@C_{80}$ in MOF-177 was calculated by inductively coupled plasma (ICP) results: ca. 5.2 mg of $DySc_2N@C_{80}$@MOF-177 crystals were dissolved in 5 ml of HNO_3, sonicated for 30 min and then transferred to a mixture of H_2SO_4/H_2O_2 (v/v = 4/1), sonicated for another 30 min. This acid solution was diluted 1000 times and detected the Dy^{3+}, Sc^{3+} and Zn^{2+} on SHIMADZU ICPE-9000 instrument. The hysteresis loops of samples were collected on a Quantum Design MPMS XL-7 system at varied temperature within ±2 T at an average field sweep rate of 3.3 mT s^{-1}. The susceptibility experiments were performed at temperature from 5 to 300 K in magnetic field of 0.1 T. The net mass of the samples is in the mg range. The samples were measured in a capsule with negligible magnetism.

2. Characterization of $DySc_2N@C_{80}$@MOF-177 complex

To verify the encapsulation of $DySc_2N@C_{80}$ into the pores of MOF-177, Powder X-ray diffraction spectrum (PXRD), transmission electron microscopy (TEM), and Specific surface area measurement (BET) and energy dispersive spectrometer (EDS) were performed. It is obvious that the PXRD spectrum of $DySc_2N@C_{80}$@MOF-177 complex is different from that of pristine MOF-177 (Figure S4a). The new peaks appearing at 2-theta value of around 6° correspond to the *d* value of about 15 Å, which is ascribed to the crystal lattice perturbation caused by $DySc_2N@C_{80}$ incarceration. Furthermore, the $DySc_2N@C_{80}$@MOF-177 complex crystal was cut off along cross section and EDS analysis was conducted (Figure S4b-S4f). It can be clearly seen that the dysprosium and scandium elements are uniformly distributed as well as carbon and zinc elements in $DySc_2N@C_{80}$@MOF-177 complex. BET surface area shows a decrease from 3672 m^2 g^{-1} in MOF-177 crystal to 1246 m^2 g^{-1} in $DySc_2N@C_{80}$@MOF-177 complex, indicating that the $DySc_2N@C_{80}$ molecules have entered into the pores of MOF-177 rather than adsorbed on the crystal surface.

3. Magnetisms of $DySc_2N@C_{80}$@MOF-177 complex with different loading amounts of $DySc_2N@C_{80}$ in MOF-177

Without $DySc_2N@C_{80}$, the MOF-177 exhibits a diamagnetic character. For 1%, 3% and 5% loading amounts of $DySc_2N@C_{80}$ in MOF-177, their similar hysteresis loops can be observed clearly on M-H curves at 5 K (see Figure S5). These results showed that the magnetization relaxation of $DySc_2N@C_{80}$ is the single-molecular property rather than the result from intermolecular interactions. The loading amount of 5% was selected to employ further investigation due to its better signal to noise ratio.

4. Supporting figures

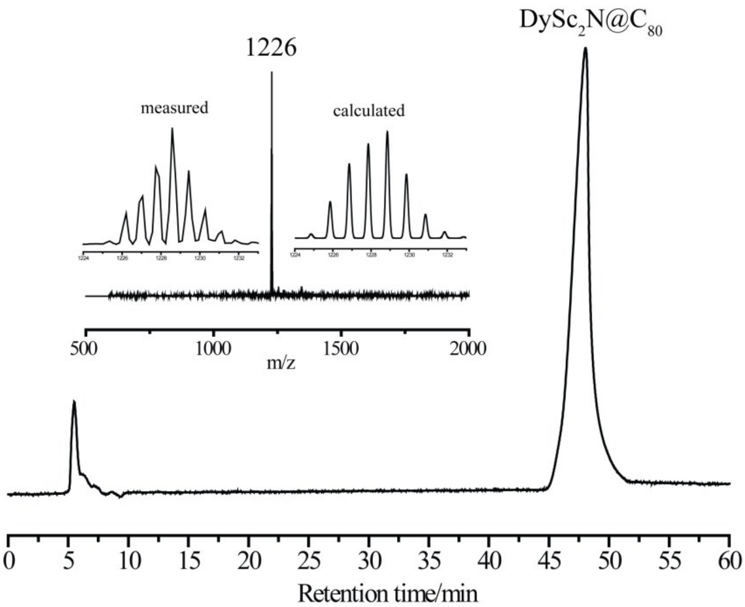

Fig S1. Chromatogram of the isolated $DySc_2N@C_{80}$. 20×250 mm Buckyprep colum, flow rate 12 mL/min and toluene as eluent. The inset shows the MALDI-TOF-MS profile of $DySc_2N@C_{80}$.

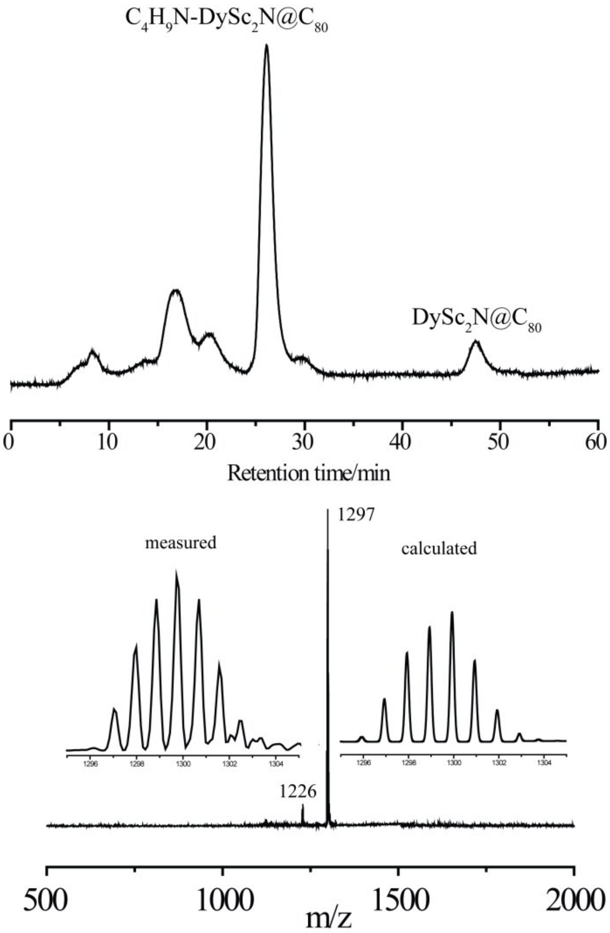

Fig S2. Chromatogram of the isolated C_4H_9N-$DySc_2N@C_{80}$. 20×250 mm Buckyprep colum, flow rate 12 mL/min and toluene as eluent. The inset shows the MALDI-TOF-MS profile of C_4H_9N-$DySc_2N@C_{80}$.

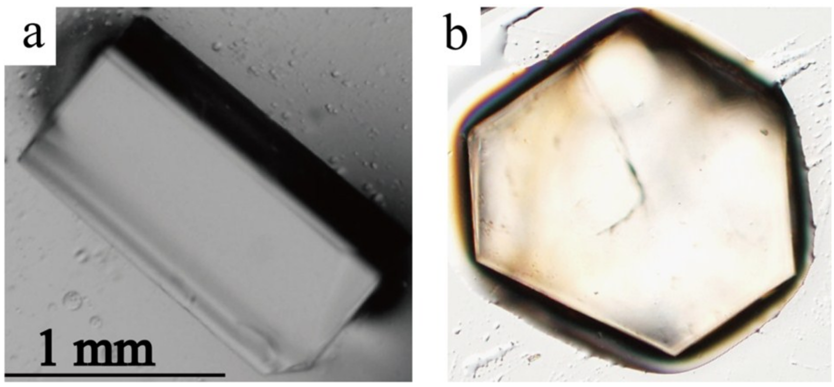

Fig S3. Optical image of as-prepared MOF-177 single crystal (a) and its cross-section (b).

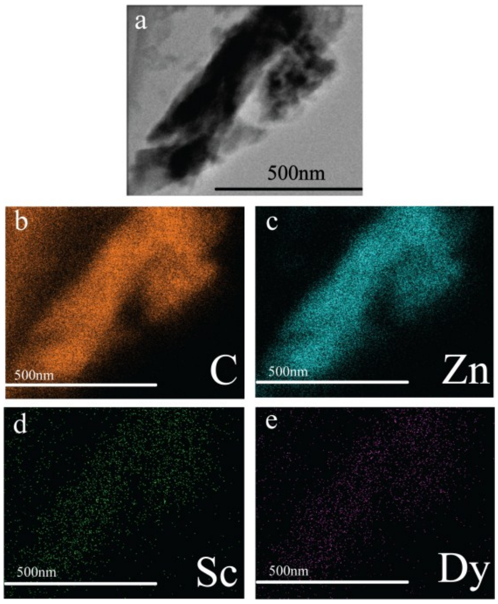

Fig S4. (a) TEM image of selected $DySc_2N@C_{80}$@MOF-177 complex. TEM element mapping of C (b), Zn (c), Sc (d) and Dy (e) for $DySc_2N@C_{80}$@MOF-177.

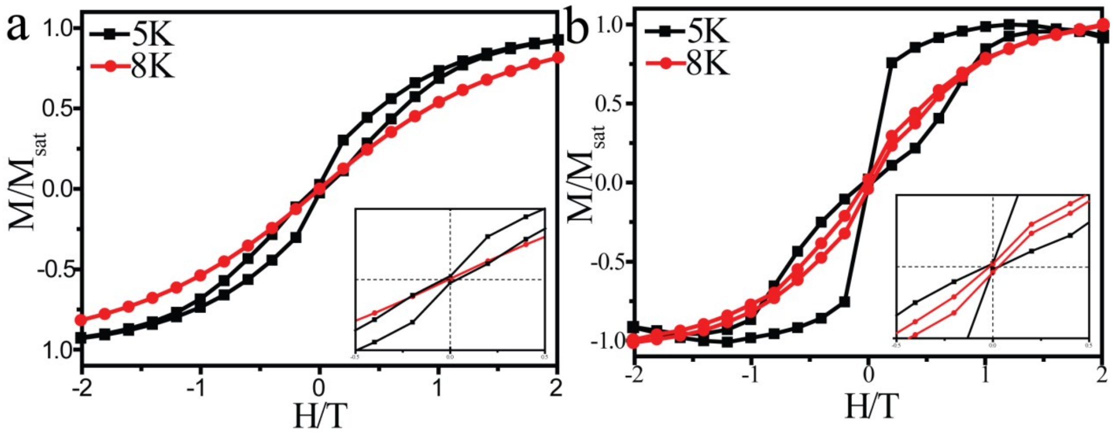

Fig S5. (a) Field-dependent hysteresis of the magnetization of $DySc_2N@C_{80}$ at 5 and 8 K. (b) Field-dependent hysteresis of the magnetization of (C_4H_9N)-$DySc_2N@C_{80}$ at 5 and 8 K.

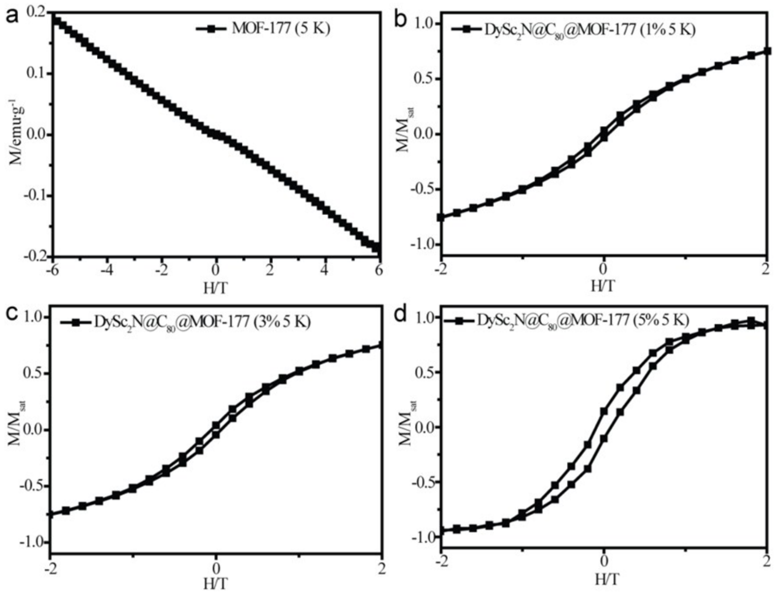

Fig S6. Field-dependent hysteresis of the magnetization at 5 K for DySc$_2$N@C$_{80}$@MOF-177 containing different weight content of DySc$_2$N@C$_{80}$. (a) 0%, (b) 1%, (c) 3%, (d) 5%, respectively.

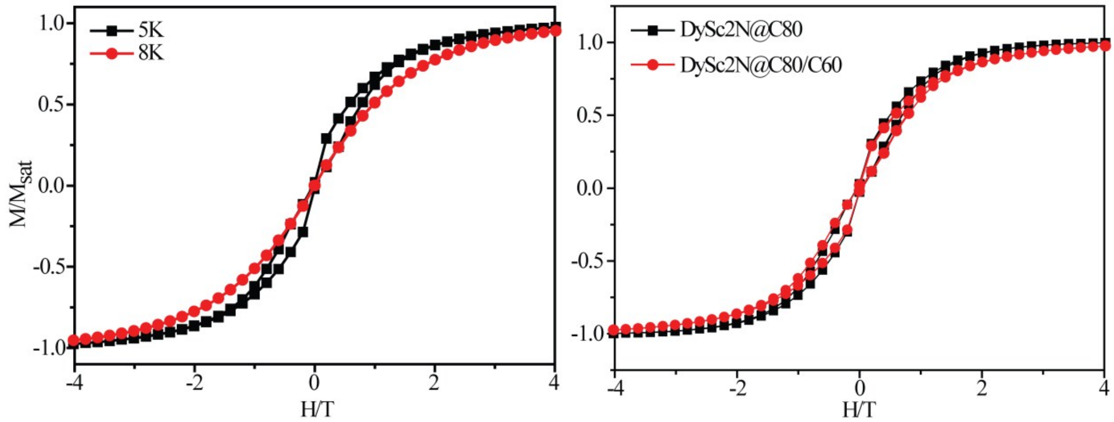

Fig S7. Field-dependent hysteresis of the magnetization for DySc$_2$N@C$_{80}$ diluted with 50 times C$_{60}$. (a) Hysteresis loops for DySc$_2$N@C$_{80}$ diluted with 50 times C$_{60}$ at 5 and 8 K. (b) Hysteresis loops for DySc$_2$N@C$_{80}$ and DySc$_2$N@C$_{80}$/C$_{60}$ mixture at 5 K.

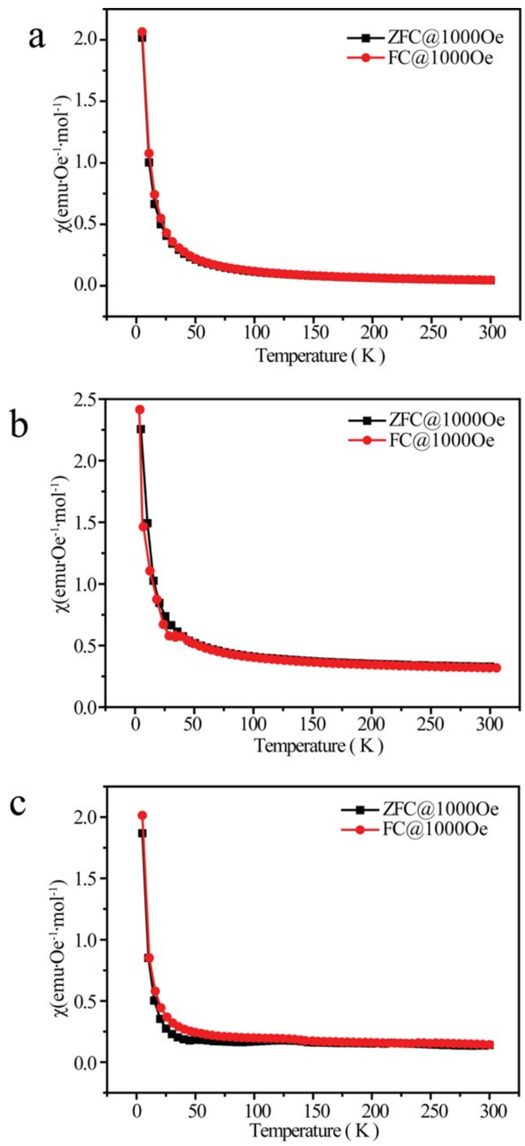

Fig S8. Temperature-dependent zero field cooled (ZFC) and field cooled (FC) susceptibilities at 1000 Oe. (a) $DySc_2N@C_{80}$ (b) C_4H_9N-$DySc_2N@C_{80}$ (c) $DySc_2N@C_{80}$@MOF-177.

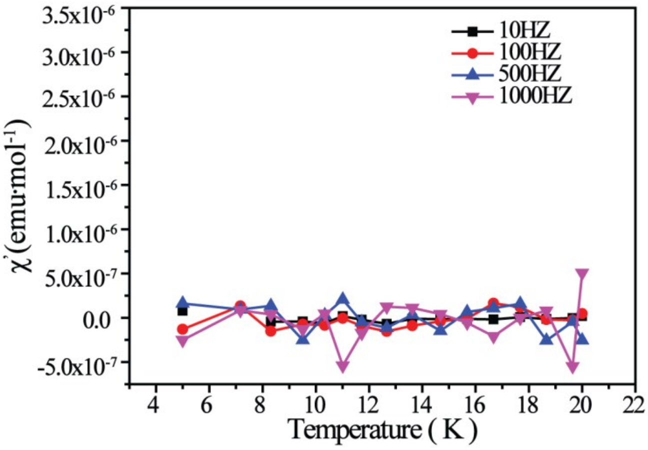

S9: The AC susceptibility of $DySc_2N@C_{80}$ powder. (The result showed the signal-noise ratio was very low and the more samples might be needed for effective data)

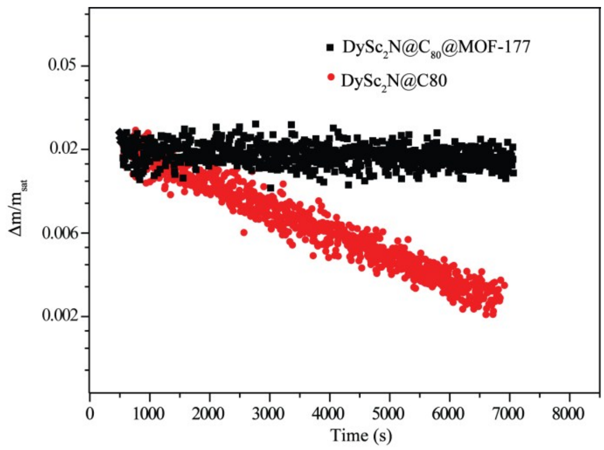

S10: Relaxation of the magnetization for $DySc_2N@C_{80}$@MOF-177 and $DySc_2N@C_{80}$ at T = 5K, with $\Delta m(t) = m(t) – m(t \rightarrow \infty)$. m_{sat} is the saturation magnetization.

5. References

1. Chae, H. K., Siberio-Perez, D. Y., Kim, J., Go, Y., Eddaoudi, M., Matzger, A. J. O'Keeffe, M., Yaghi, O. M, *Nature* **2004**, 427, 523-527.